Acta Crystallographica Section F
Structural Biology and Crystallization Communications
ISSN 1744-3091
Editors: **H. M. Einspahr and M. S. Weiss**

Cloning, purification, crystallization and X-ray crystallographic analysis of *Ignicoccus hospitalis* neelaredoxin

Filipa G. Pinho, Célia V. Romão, Ana F. Pinto, Lígia M. Saraiva, Harald Huber, Pedro M. Matias, Miguel Teixeira and Tiago M. Bandeiras

Acta Cryst. (2010). F**66**, 605–607

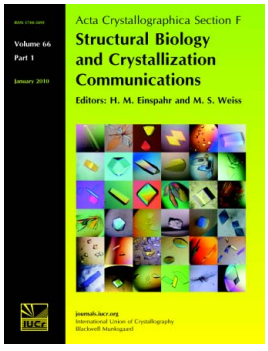

Acta Crystallographica Section F
Structural Biology and Crystallization Communications
ISSN 1744-3091

Cloning, purification, crystallization and X-ray crystallographic analysis of *Ignicoccus hospitalis* neelaredoxin

Filipa G. Pinho,[a] Célia V. Romão,[b] Ana F. Pinto,[b] Lígia M. Saraiva,[b] Harald Huber,[c] Pedro M. Matias,[b] Miguel Teixeira[b] and Tiago M. Bandeiras[a]*

[a]Instituto de Biologia Experimental e Tecnológica, Apartado 12, 2701-901 Oeiras, Portugal, [b]Instituto de Tecnologia Química e Biológica, Universidade Nova de Lisboa, Apartado 127, 2781-901 Oeiras, Portugal, and [c]Lehrstuhl für Mikrobiologie, Universität Regensburg, 93053 Regensburg, Germany

Correspondence e-mail: tiagob@itqb.unl.pt

Received 24 February 2010
Accepted 30 March 2010

Superoxide reductases (SORs) are metalloproteins which constitute the most recently identified oxygen-detoxification system in anaerobic and microaerobic bacteria and archaea. SORs are involved in scavenging superoxide radicals from the cell by catalyzing the reduction of superoxide ($O_2^{\bullet-}$) to hydrogen peroxide and are characterized by a catalytic nonhaem iron centre coordinated by four histidine ligands and one cysteine ligand. *Ignicoccus hospitalis*, a hyperthermophilic crenarchaeon, is known to have a neelaredoxin-type SOR that keeps toxic oxygen species levels under control. Blue crystals of recombinant *I. hospitalis* oxidized neelaredoxin (14.1 kDa, 124 residues) were obtained. These crystals diffracted to 2.4 Å resolution in-house at room temperature and belonged to the hexagonal space group $P6_222$ or $P6_422$, with unit-cell parameters $a = b = 108$, $c = 64$ Å. Cell-content analysis indicated the presence of one monomer in the asymmetric unit.

1. Introduction

All lifeforms require protection mechanisms against reactive oxygen species, which are produced upon the partial reduction of molecular oxygen. Furthermore, oxygen in itself is also toxic to anaerobic organisms. The superoxide anion ($O_2^{\bullet-}$) is one of the reactive oxygen species that are formed upon one-electron reduction of O_2 and in many organisms is detoxified by superoxide dismutases (SODs), which couple the oxidation and reduction of superoxide anion (McCord & Fridovich, 1969),

$$M^{n+} + O_2^{\bullet-} \rightarrow M^{(n-1)+} + O_2 \quad (1)$$

$$M^{(n-1)+} + O_2^{\bullet-} \rightarrow M^{n+} + H_2O. \quad (2)$$

Superoxide reductases (SORs) constitute a new family of enzymes that are able to scavenge superoxide anion through its reduction only (2) (Jenney *et al.*, 1999; Pinto *et al.*, 2010), which distinguishes them from the SODs. Superoxide reductases have so far only been found in anaerobic and microaerobic organisms.

SORs can be classified as 1Fe-SORs (or neelaredoxins) or 2Fe-SORs (or desulfoferrodoxins) according to the number of metal centres. Both share a common active site in which the reduction of superoxide anion occurs. This site is composed of a pentacoordinated iron with four equatorial histidine imidazoles and one axial cysteine sulfur in a square-pyramidal geometry [Fe(Cys)(His)$_4$]. In the oxidized state, and in most SORs, a glutamate residue near the iron centre is coordinated to the other axial position of the iron, resulting in an octahedral geometry. In the reduced state the glutamate residue no longer coordinates to the iron, allowing $O_2^{\bullet-}$ to bind (Pinto *et al.*, 2010). The active-site-containing domain adopts a seven-stranded β-barrel immunoglobin-like fold. In 2Fe-SORs this β-barrel domain is linked by a loop to an N-terminal domain containing a second iron centre: a desulforedoxin-like centre, *i.e.* an Fe atom coordinated by four cysteine sulfurs in a distorted tetrahedral geometry $[Fe(Cys)_4]^{3+}$ (Archer *et al.*, 1995; Coelho *et al.*, 1997). The function of this additional iron centre has still not been clarified but it is known not to be crucial for superoxide reduction. Interestingly, this extra N-terminal

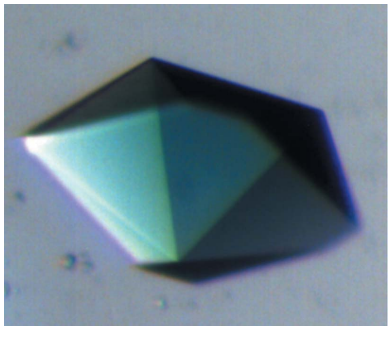

domain was also found in *Treponema pallidum* SOR, which lacks the cysteine motif for iron binding (Pereira *et al.*, 2007).

Ignicoccus hospitalis, a chemolithoautotrophic and hyperthermophilic crenarchaeon isolated from a submarine hydrothermal system at the Kolbeinsey Ridge (north of Iceland), is the only organism known to date that is capable of acting as a host for *Nanoarchaeum equitans*, the only cultivated member of the Nanoarchaeota (Paper *et al.*, 2007; Huber *et al.*, 2000). The SOR protein encoded in the *I. hospitalis* genome is a 1Fe-SOR (*Ih* Nlr) and its amino-acid sequence shows the 'conserved' motif E_{23}**K**H**V**P_{27}, apart from the lysine and valine residues shown in bold, which are both replaced by threonine residues (Podar *et al.*, 2008). The positively charged amino-acid lysine, which was thought to be conserved, has been proposed to play a key role in the catalytic cycle of superoxide reduction, namely by attracting the anionic substrate and creating a positively charged surface around the catalytic site (Lombard *et al.*, 2001). The absence of this lysine residue in *I. hospitalis* SOR is relevant to understanding its role in the catalytic reaction and discriminating the essential amino-acid residues for superoxide reduction.

In this study, we describe the cloning, purification, crystallization and preliminary X-ray crystallographic analysis of the 1Fe-SOR from *I. hospitalis*. Its crystal structure will contribute to clarification of the superoxide-reduction mechanism.

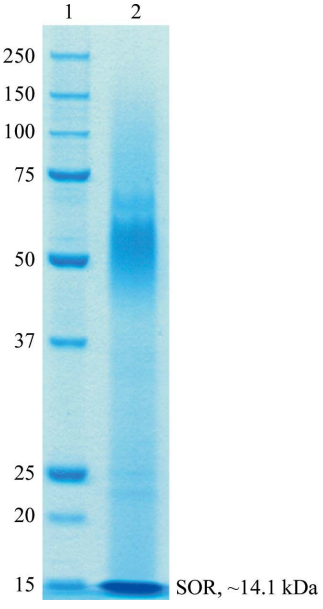

Figure 1
SDS–PAGE (10%) gel of pure recombinant *Ih* Nlr. Lane 1, BioRad unstained protein markers (labelled in kDa); lane 2, *Ih* Nlr (SOR) monomer migrating according to the expected molecular mass of 14.1 kDa.

2. Experimental procedures and results

2.1. Cloning and protein overproduction

Amplification of the complete *nlr* gene sequence (375 bp) encoding the neelaredoxin from *I. hospitalis* was achieved by PCR using genomic DNA of *I. hospitalis* and primers 5′-GAG GAC ACG GAC GAG CAT ATG AAG AG-3′ (including an *Nde*I restriction site) and 5′-GAG GGA GAA CGA AGC TTT TTC CTT TC-3′ (including a *Hin*dIII restriction site). The DNA fragment obtained was then cloned into the vector pET24a (+) (Novagen), transformed first into *Escherichia coli* XL2Blue cells. After sequencing to confirm the absence of unwanted mutations, the recombinant plasmid was transferred into *E. coli* strain BL21 (DE3) Gold. The cells were grown aerobically at 310 K in M9 minimal medium (da Costa *et al.*, 2003) supplemented with 30 µg ml^{-1} kanamycin and enriched with 200 µ*M* $FeSO_4{\cdot}7H_2O$ until the $OD_{600\,nm}$ reached 0.3. At this stage, 400 µ*M* isopropyl *β*-D-1-thiogalactopyranoside was added, the temperature was lowered to 301 K and growth continued for 20 h. The cells were then harvested by centrifugation at 10 000*g* for 10 min at 277 K.

2.2. Purification

Harvested cells were resuspended in a buffer containing 20 m*M* Tris–HCl pH 7.6, 1 m*M* phenylmethanesulfonyl fluoride (PMSF) and 20 µg ml^{-1} DNase (Sigma), and broken in a minicell French press at 131 MPa. All subsequent purification steps were performed at pH 7.6 and 277 K. After centrifugation at 100 000*g* for 2 h, the soluble extract was dialyzed against 20 m*M* Tris–HCl and 1 m*M* PMSF (buffer *A*), heated at 333 K for 20 min and centrifuged at 7000*g* for 20 min. The soluble fraction was subsequently loaded onto a Q-Sepharose Fast Flow column (XK 26/10; GE Healthcare) previously equilibrated with buffer *A*. The fraction containing *Ih* Nlr eluted in the flowthrough; it was concentrated by ultrafiltration (Amicon, 10 kDa cutoff) and loaded onto a Superdex 75 column (XK 26/60; GE Healthcare) equilibrated with 20 m*M* Tris–HCl and 150 m*M* NaCl. The collected fractions were analyzed and judged to be pure on the basis of SDS–PAGE gels (Fig. 1). The protein concentration and total iron content were determined using the bicinchoninic acid protein-assay kit (Pierce; Smith *et al.*, 1985) and the 2,4,6-tripyridyl-*S*-triazine method (Fisher & Price, 1964), respectively. Finally, the protein was concentrated to 15 mg ml^{-1} using a 10 kDa cutoff Centricon (Vivaspin).

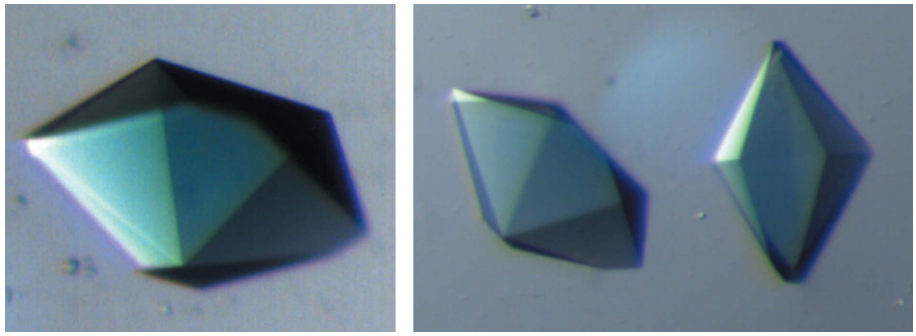

Figure 2
Crystals of *I. hospitalis* neelaredoxin grown in 85 m*M* Tris–HCl pH 8.5, 8.5 m*M* $NiCl_2$, 15%(*v*/*v*) PEG 2000 monomethyl ether and 15%(*v*/*v*) glycerol. The largest crystal dimensions are ∼350 × 200 × 200 µm.

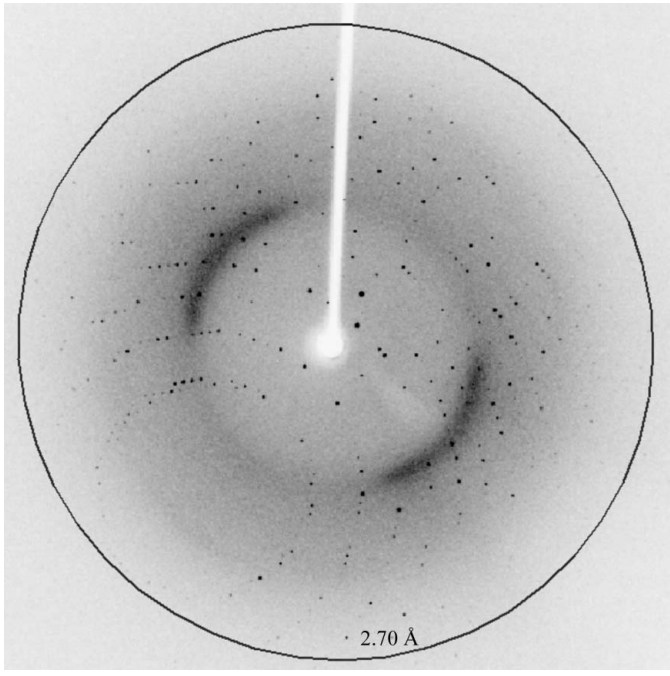

Figure 3
Diffraction image of an *I. hospitalis* neelaredoxin crystal collected in-house at room temperature.

2.3. Crystallization and cryoprotection

Initial crystallization screening was performed using a protein concentration of 15 mg ml^{-1} in 20 m*M* Tris–HCl pH 7.2, 150 m*M* NaCl. Screening was carried out with the NeXtal/Qiagen Classics I screen using the sitting-drop vapour-diffusion method in a 96-well plate (Greiner) and a Cartesian Minibee nanolitre robot (Genomics Solutions). Three different drop ratios were prepared per condition screened, using 100:100 nl, 100:200 nl and 200:100 nl ratios of reservoir and protein solution. The drops were equilibrated against 100 µl reservoir solution. After 2 h equilibration, promising protein crystals were obtained from conditions 22 [0.1 *M* HEPES pH 7.5, 70%(*v*/*v*) MPD] and 82 [0.1 *M* Tris pH 8.5, 0.01 *M* $NiCl_2$, 20%(*v*/*v*) PEG 2000 monomethyl ether]. The crystals from the first condition were light blue multiple plate-like crystals with a hexagonal shape, while those from the second condition were dark blue, single, thick and hexagonal bipyramid-shaped. Both conditions were manually reproduced and optimized in 24-well plates using the hanging-drop vapour-diffusion method and the best crystals were obtained from optimization of condition 82. Hexagonal bipyramid-shaped crystals with maximum dimensions of 350 × 200 × 200 µm were obtained using a crystallization solution consisting of 85 m*M* Tris pH 8.5, 8.5 m*M* $NiCl_2$, 15%(*v*/*v*) PEG 2K MME and 15%(*v*/*v*) glycerol in drops composed of 2 µl protein and 0.5 µl reservoir solution (Fig. 2). Owing to the high sensitivity of the *Ih* Nlr crystals to the most common cryoprotectants (*e.g.* glycerol, PEG 400 and ethylene glycol), eight different cryoprotectants were tested, but without success: 20% MPD, 1 *M* sodium malonate, 17.5% sucrose, 1 *M* ammonium sulfate, 17.5% 2-propanol, 3.5 *M* sodium nitrate and 2 *M* magnesium acetate.

2.4. Data collection and processing

Since no suitable cryoprotectant could be found, X-ray diffraction data were collected in-house at room temperature. One crystal was mounted on a MiTeGen MicroMount steel pin glued to a MiTeGen MicroRT capillary-mounting system. A 2.4 Å resolution diffraction data set was measured using a Bruker AXS Proteum Pt135 CCD detector system coupled to a Bruker AXS Microstar-I rotating-anode X-ray generator with Montel mirrors (see Fig. 3). The images were processed with *SAINT* and scaled with *SADABS* as part of the Bruker AXS *PROTEUM* software suite. The quality of the diffraction data was analyzed using *XPREP* (Bruker AXS) and a summary of the statistics is presented in Table 1. Work is in progress towards establishing cryoconditions that will allow flash-cooled crystals to be measured at a synchrotron X-ray source in order to obtain a data set to the highest possible resolution.

Table 1
Diffraction data-collection and processing parameters.

Wavelength (Å)	1.5418
Space group	$P6_222$ or $P6_422$
Unit-cell parameters (Å)	$a = b = 108.3$, $c = 64.46$
Resolution range (Å)	41.5–2.39 (2.45–2.39)
Scan type	ω
Total angular range† (°)	125.75
Total No. of frames†	503
Exposure time per frame (s)	60
No. of observations	101709 (1494)
Unique reflections	16568 (799)
$\langle I/\sigma(I)\rangle$	14.61 (1.11)
$R_{\rm merge}$‡ (%)	8.6 (73.2)
$R_{\rm p.i.m.}$§ (%)	3.7 (46.8)
Completeness (%)	99.1 (85.4)
Multiplicity	6.08 (1.87)
Wilson *B* factor (Å^2)	34.7
No. of molecules in asymmetric unit	1
$V_{\rm M}$ (Å^3 Da^{-1})	3.90
Estimated solvent content (%)	68.4

† In two different crystal settings. ‡ $R_{\rm merge} = \sum_{hkl}\sum_i |I_i(hkl) - \langle I(hkl)\rangle| / \sum_{hkl}\sum_i I_i(hkl)$. § $R_{\rm p.i.m.} = \sum_{hkl}[1/(N-1)]^{1/2}\sum_i |I_i(hkl) - \langle I(hkl)\rangle| / \sum_{hkl}\sum_i I_i(hkl)$, where $I_i(hkl)$ is the observed intensity, $\langle I(hkl)\rangle$ is the average intensity of multiple observations of symmetry-related reflections and N is their redundancy.

This work was supported by Fundação para a Ciência e Tecnologia Project PTDC/BIA-PRO/67263/2006. AFP is the recipient of an FCT grant (SFRH/BD/41355/2007). FGP is the recipient of an IBET fellowship.

References

Archer, M., Huber, R., Tavares, P., Moura, I., Moura, J. J., Carrondo, M. A., Sieker, L. C., LeGall, J. & Romao, M. J. (1995). *J. Mol. Biol.* **251**, 690–702.
Coelho, A. V., Matias, P., Fülöp, V., Thompson, A., Gonzalez, A. & Carrondo, M. A. (1997). *Biol. Inorg. Chem.* **2**, 680–689.
da Costa, P. N., Teixeira, M. & Saraiva, L. M. (2003). *FEMS Microbiol. Lett.* **218**, 385–393.
Fisher, D. S. & Price, D. C. (1964). *Clin. Chem.* **10**, 21–31.
Huber, H., Burggraf, S., Mayer, T., Wyschkony, I., Rachel, R. & Stetter, K. O. (2000). *Int. J. Syst. Evol. Microbiol.* **50**, 2093–2100.
Jenney, F. E. Jr, Verhagen, M. F., Cui, X. & Adams, M. W. (1999). *Science*, **286**, 306–309.
Lombard, M., Houée-Levin, C., Touati, D., Fontecave, M. & Nivière, V. (2001). *Biochemistry*, **40**, 5032–5040.
McCord, J. M. & Fridovich, I. (1969). *J. Biol. Chem.* **244**, 6049–6055.
Paper, W., Jahn, U., Hohn, M. J., Kronner, M., Nather, D. J., Burghardt, T., Rachel, R., Stetter, K. O. & Huber, H. (2007). *Int. J. Syst. Evol. Microbiol.* **57**, 803–808.
Pereira, A. S., Tavares, P., Folgosa, F., Almeida, R. M., Moura, I. & Moura, J. J. G. (2007). *Eur. J. Inorg. Chem.* **2007**, 2569–2581.
Pinto, A. F., Rodrigues, J. V. & Teixeira, M. (2010). *Biochim. Biophys. Acta*, **1804**, 285–297.
Podar, M. *et al.* (2008). *Genome Biol.* **9**, R158.
Smith, P. K., Krohn, R. I., Hermanson, G. T., Mallia, A. K., Gartner, F. H., Provenzano, M. D., Fujimoto, E. K., Goeke, N. M., Olson, B. J. & Klenk, D. C. (1985). *Anal. Biochem.* **150**, 76–85.